Fission of Radium by 11- to 22-Mev Protons*

ROBERT L. WOLKE†
Department of Chemistry, University of Florida, Gainesville, Florida
(Received June 1, 1960)

The ranges and relative yields of Sr^{91} and Pd^{112} fragments from the fission of Ra^{226} by 11- to 22-Mev protons were determined by a radiochemical recoil-catching technique. The relative yield data indicate that above 11 Mev the three-humped mass-yield curve becomes predominantly "symmetric" and perhaps somewhat narrower. An apparent fission threshold of ~10.4 Mev was observed. The curve of total fission yield vs energy has the same slope between 13 and 22 Mev as has been reported for the fast-neutron-induced fission of radium. The ranges in mg Au/cm² at 11 and 20 Mev, respectively, are, Sr^{91}: 11.2±0.9 and 10.8±0.2; Pd^{112}: 9.1±1.0 and 9.2±0.3, corresponding to an average total kinetic energy of 162±10 Mev.

I. INTRODUCTION

SEVERAL studies have shown that in general, as one increases the kinetic energy of a particle incident on a high-Z^2/A nucleus, the mass-yield curve for fission changes gradually from a two-humped, asymmetric configuration to a one-humped, symmetric one. Furthermore, as one chooses successively lighter targets at the same relatively low excitation energy, the light asymmetric hump tends to move away from the heavy asymmetric hump. It might be expected then, that if a target could be chosen which has a high enough Z^2/A to fission asymmetrically at a relatively low energy, yet is light enough so that its asymmetric humps are well-separated, the mass-yield curves within some small region of incident-particle energy might display the contribution of symmetric fission as a separate peak lying between the asymmetric humps. The fission of Ra^{226} by 11-Mev protons has been found by Jensen and Fairhall[1] to exhibit such a three-humped mass-yield curve, in which the symmetric and asymmetric peak yields are roughly equal. The same authors[2] have recently observed a three-humped mass-yield curve for 14.5-Mev deuterons on radium. Some preliminary data[3] indicate that the photofission of Ra^{226} by 23-Mev bremsstrahlung may also be consistent with a three-humped mass-yield curve.

Although the shapes of these curves can in some ways be correlated with well-established trends in fission asymmetry, studies of the fission of radium as a function of energy might be expected to shed light on the mechanism or mechanisms involved.

Measurements of the peak symmetric and asymmetric yields alone can indicate changes in the shape of the mass-yield curve, while the measurement of fragment ranges can, in principle, give information on the energetics of the fission process. Sr^{91} and Pd^{112}, the principal light asymmetric and symmetric fragments, respectively, were chosen as the subjects of the present experiments.

II. EXPERIMENTAL METHOD

The ranges and relative yields of Sr^{91} and Pd^{112} fragments were determined by a stacked foil experiment, with radiochemical separation of the recoiling fission fragments from Au or Al absorbers and recoil catchers. The radium target[4] is shown in Fig. 1. It consists of a $2\frac{7}{16}$-in. disk of 5-mil Ag foil with an active coating, approximately 1 in. square, on each face. The active coating is composed of three layers of gold: a half-micron undercoating, a 1.5-micron target layer loaded with about a milligram of $RaSO_4$, and a half-micron protective overcoating to minimize emanation. The 1-mil Al foil masks, which were placed next to the target faces in all runs, limited the observed recoils to those arising only from the central half-inch diameter area of each active coating. Radioautographs of the target faces showed no obvious inhomogeneities in radium distribution over the active layers.

The target and recoil-catcher foils were stacked

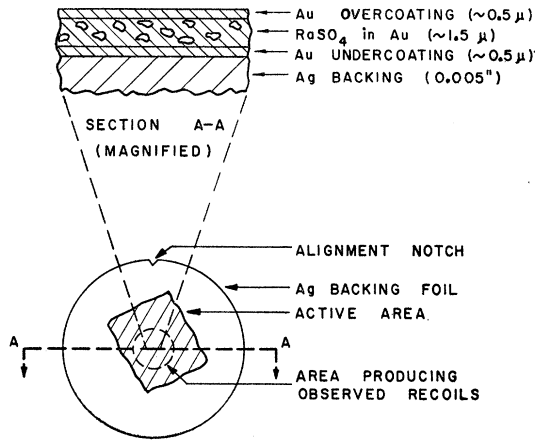

FIG. 1. Radium-loaded target foil.

* Much of this work was done under a Research Participation contract with the Oak Ridge Institute of Nuclear Studies and under a subcontract with the Electronuclear Research Division of Oak Ridge National Laboratory, operated for the U. S. Atomic Energy Commission by the Union Carbide Nuclear Corporation.

† Present address: Department of Chemistry, University of Pittsburgh, Pittsburgh 13, Pennsylvania.

[1] R. C. Jensen and R. W. Fairhall, Phys. Rev. **109**, 942 (1958).

[2] R. C. Jensen and R. W. Fairhall, Phys. Rev. **118**, 771 (1960).

[3] R. B. Duffield, R. A. Schmitt, and R. A. Sharp, *Proceedings of the Second United Nations International Conference on the Peaceful Uses of Atomic Energy, Geneva, 1958* (United Nations, Geneva, 1958), Vol. 15, p. 202.

[4] Prepared to specifications by the U. S. Radium Corporation.

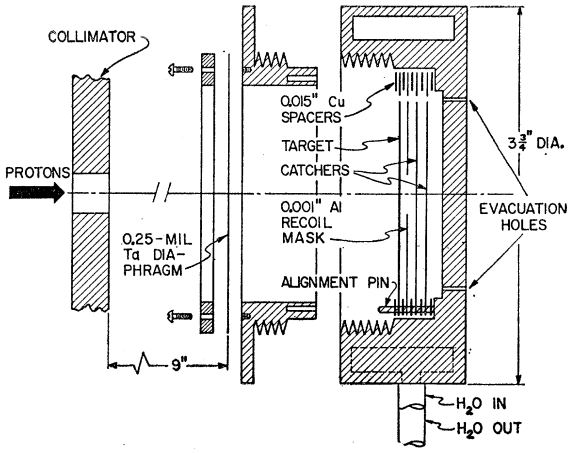

FIG. 2. Target and foil-stack holder.

together in the cylindrical, 2*S*-aluminum holder which is shown exploded in Fig. 2. A target foil, a mask, and two catchers are shown in place in the holder. The copper spacing rings prevented any damaging contact between the fragile Au foils. The thin Ta diaphragm was included to minimize the spread of radioactivity should the Ra targets melt in the beam. Temperature measurements showed, however, that the cooling water circulating through the annular channel shown in Fig. 2 kept the maximum temperature of the foils below 70°C during the bombardments. The loaded holder was bombarded with a ½-inch collimated beam of 22-Mev protons for about two hours in the evacuated 4-inch external beam pipe of the ORNL 86-inch cyclotron. The irradiations were monitored roughly by integrating the proton current incident on the thick back wall of the target holder. Beam intensities were typically about 10 μa.

After a cooling period of 10 or 12 hours, the Au or Al recoil-catchers were dissolved in aqua regia. After the addition of holdback carriers for Sr and Pd, the gold was removed by extraction into isoamyl acetate. An initial precipitation of palladium dimethylglyoxime (DMG) was then used to separate Pd from Sr. The Pd was then isolated in pure form by a series of successive DMG and scavenging precipitations, while the Sr fraction was purified by several precipitations from fuming HNO_3 and by scavenging with $Fe(OH)_3$ and $BaCrO_4$. The latter was effective in removing Ra contamination. The final precipitates of $Pd(DMG)_2$ and $SrCO_3$ were mounted on cardboard under Mylar and counted by methane-flow proportional counters.

Both differential and integral range experiments were done. Fig. 3(a) shows the arrangement for a differential experiment. Fission fragments recoiling from the target in the forward hemisphere penetrated a series of thin Au absorbers, from each of which the desired fragments were separated and counted to determine the differential range curve (counts/min per mg/cm² vs mg/cm² absorber). Backward recoils were caught on the thick Al "integral catcher," from which the relative yields were determined. After the differential range curves had been determined approximately by this method, the "integral" experiments shown in Fig. 3(b) were employed to define the ranges more accurately. These integral experiments consisted essentially of the Douthett-Templeton two-foil method,[5] modified for targets of intermediate thickness as explained in Sec. III B, below. The fission fragment ranges could thus be determined from the ratio of activities found in foils *a* and *b*. The effects of two different proton energies were studied simultaneously by placing targets T_1 and T_2 on either side of the proton energy-degrading Al absorber. As in the differential experiments of Fig. 3(a), the thick "integral catchers" caught all recoils in the backward hemisphere for relative yield determinations.

The activities of all samples were followed for approximately forty hours after completion of the chemistry. Sr and Pd activities were compared at 30 and 48 hours, respectively, after the end of the irradiation. Analysis of some extended decay curves showed that at these comparison times the detected radiations comprised about 90% Sr^{91} or Pd^{112}. No corrections were made for self-absorption since in any given run the sample thicknesses varied by no more than ~1 mg/cm², and fluctuations were partly averaged out over the five duplicate integral experiments which were done. Other counting corrections were unnecessary because the experimental results depend on ratios of activities.

Several possible sources of extraneous activity were

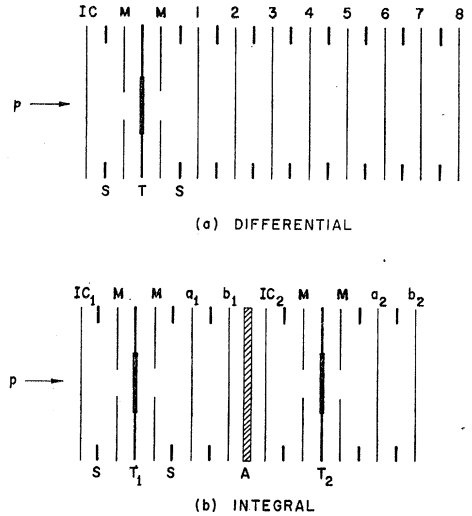

FIG. 3. Exploded views of the foil stacks used for the differential and integral range experiments. *IC*=integral catcher, *M*=mask (0.001-in. Al), *T*=target, 1–8=differential absorbers (1.7 mg Au/cm²), *S*=spacer (0.015-in. Cu), *a*=first absorber (1.7 mg Au/cm²), *b*=second absorber (1-mil Al), *A*=proton absorber (Al). Subscripts 1 and 2 refer to the higher and lower proton energies, respectively.

[5] E. M. Douthett and D. H. Templeton, Phys. Rev. **94**, 128 (1954).

investigated. Neutron-induced fission effects were sought by irradiating a target behind an Al absorber which was just thick enough to stop all protons. Catchers on either side of the target showed no detectable Sr or Pd activity after the standard cooling period and chemistry. A similar experiment with a silver foil target showed no Pd activity from the $Ag^{109}(n,p)Pd^{109}$ reaction, assuring that the silver foil target-backing was substantially inert during the fission runs. Interference from the fission of Au was investigated by irradiating a stack of eight standard (0.000 031-in. thick) Au absorbers and separating a single Sr fraction from the entire stack. Only a few counts/min. above background were found, indicating that Au interference in the normal runs was roughly 0.1%, which is less than the experimental error. A set of thicker (0.00010-in.) Au foils from the same supplier,[6] however, were found to produce significant amounts of both Sr and Pd activities from reactions of impurities. These foils were not used in the Ra runs. As a final check for interfering activities, a dummy target, identical to the fission targets except that it contained no $RaSO_4$ in the middle Au layer, was irradiated in the same way as for a fission run. No Sr or Pd activities were detectable in adjacent Al catchers.

The 0.000 031-inch (1.7 mg/cm^2) Au foils used as recoil catchers were obtained as 4×4 in. square sheets. Measurements showed their areas to be reproducible to an average deviation of 0.2%. The thickness of each foil used in the experiments was therefore determined by weighing, which gave the thickness to a precision of ±0.003 mg/cm^2. Each catcher was prepared for use by gluing it tautly onto a Cu spacer ring. The foil area inside the ring, i.e., the area which could conceivably receive recoils during the run, constituted 16% of the weighed sheet. It was assumed, and roughly substantiated by visual checks for pinholes and thin spots, that this 16% was of the same average thickness as the whole weighed sheet.

The energy of the incident proton beam during the experiments was 22.4±0.6 Mev.[7] This nominal value was used in computing the mean proton energy at any point in the target stack from the range-energy data of Aron, Hoffman, and Williams[8] and Bichsel.[9] Loss of protons by scattering during traversal of absorbers was assumed to be negligible.

III. TREATMENT OF DATA

A. Relative Yields

The relative yields of Sr^{91}, Pd^{112}, and total fission were determined as a function of proton energy by counting the backward-hemisphere recoils in the "integral catchers" described above. Because of possible variations in center-of-mass motion and in fission anisotropy with proton energy, the backward-hemisphere yield of a given fragment may not remain strictly proportional to the total yield as the proton energy is varied. Even if one assumes completely inelastic momentum transfer from the proton to the Ra^{226} target, however, the ratio η of the fissioning-nucleus velocity to the velocity of a fragment in the c.m. system is only of the order of 0.018. Moreover, η can be expected to remain fairly constant over the small range of proton energies used in the present work. Only a serious energy dependence of the shape of the c.m. angular distribution, then, could prevent the measured yields from being proportional to the true yields of Sr^{91} or Pd^{112} over the investigated energy interval. The validity of the total fission yield data will be discussed in Sec. IV A, below.

B. Ranges

The thickness of the fission fragment recoil sources (i.e., the Ra-Au targets) in the present experiments was some 20 to 30% of the fragment ranges. The usual thin- or thick-source range treatments do not, therefore, apply. We shall consider the intermediate-thickness case as it applies first to the differential range measurements and then to the integral, or two-foil, method. In the following derivations, an isotropic c.m. angular distribution and $\eta=0$ are assumed for simplicity. The existence of an η of ≤ 0.018 would affect the results less than the experimental error, while the equations are relatively insensitive to anisotropy.

Consider a plane source of thickness nR, where $0\leq n\leq 1$, emitting recoils of range R into a large, adjacent absorber of the same material and of thickness t [Fig. 4(a)]. Of all the recoils which originate at a depth x in the source, the fraction $N(>t)$ which succeed in completely penetrating the absorber is proportional to the fractional solid angle subtended by the cone whose half-angle $\theta=\arccos[(t+x)/R]$. That is, $N(>t)$ is proportional to the integral of $\sin\theta d\theta$ from 0 to $\arccos[(t+x)/R]$ for a given x. This function is then to be integrated over x in the two distinct regions of t:

$$N(>t)=k\int_0^{nR}\int_0^{\arccos[(t+x)/R]}\sin\theta d\theta dx \qquad (1)$$

for $t\leq R(1-n)$ (Region I), and

$$N(>t)=k\int_0^{R-t}\int_0^{\arccos[(t+x)/R]}\sin\theta d\theta dx \qquad (2)$$

for $R(1-n)\leq t\leq R$ (Region II), where k is a constant depending on cross section, target mass and density, beam intensity, and numerical factors. Integration of Eqs. (1) and (2) yields

$$N(>t)=knR(1-n/2-t/R) \qquad (3)$$

[6] Hastings and Company, Inc., Philadelphia, Pennsylvania.
[7] J. L. Need (private communication).
[8] W. A. Aron, B. G. Hoffman, and F. C. Williams, Atomic Energy Commission Report AECU-663, 1949 (unpublished).
[9] H. Bichsel, Phys. Rev. 112, 1089 (1958).

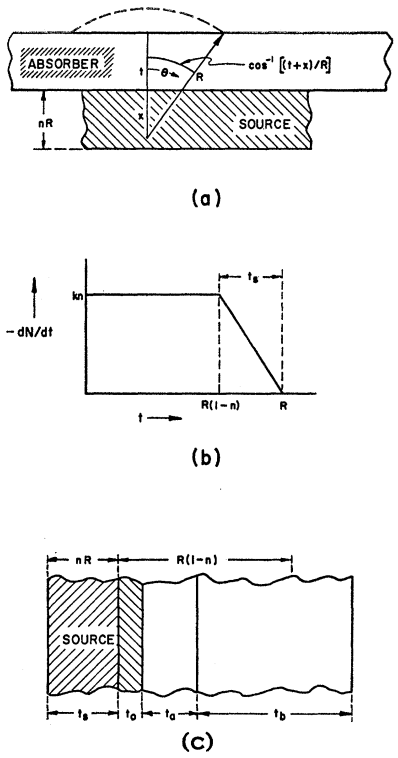

FIG. 4. (a) Intermediate-thickness source of recoils and an adjacent absorber of the same material. (b) Differential range curve from an intermediate-thickness source. Range straggling effects are not included. (c) Integral (two-foil) range experiment, showing source with overcoating and two absorbers. See text.

in Region I and

$$N(>t)=\tfrac{1}{2}kR(1-t/R)^2 \tag{4}$$

in Region II. The number $-dN$ of fragments stopped in a thickness element dt at any depth in the absorber can be obtained by differentiating Eqs. (3) and (4). Thus,

$$-dN=kndt \tag{5}$$

in Region I and

$$-dN=k(1-t/R)dt \tag{6}$$

in Region II. A plot of $-dN/dt$ vs t from Eqs. (5) and (6), which constitutes a differential range curve, is shown in Fig. 4(b). In actuality, the sharp breaks at $t=R(1-n)$ and $t=R$ are rounded off by range straggling, as will be seen in the experimental curve shown below.

The two-foil method of Douthett and Templeton[5] can be modified for a source of intermediate thickness by the following considerations. Fig. 4(c) shows the experimental situation, in which a source of thickness $t_s=nR$ with an overcoating of thickness t_0 emits fragments into two adjacent absorbers of thicknesses t_a and t_b. The thickness t_a is chosen so that $t_0+t_a<R(1-n)$, while t_b is infinitely thick to the fragments. [In practice, t_0+t_a must be thin enough so that it includes no range straggling effects in the vicinity of $R(1-n)$.] Thus the first absorber is entirely within Region I and the second absorber covers the rest of Region I and all of Region II. The number N_a of fragments ending their ranges in the first absorber is given by Eq. (5) as

$$N_a=kntₐ. \tag{7}$$

The number N_b of fragments stopped in the second absorber is simply the number of fragments which penetrate beyond $t=t_0+t_a$. Equation (3) gives

$$N_b=kn(R-nR/2-t_0-t_a). \tag{8}$$

Finally, combination of Eqs. (7) and (8), remembering that $t_s=nR$, yields

$$R=t_s/2+t_0+t_a(1+N_b/N_a). \tag{9}$$

The range, therefore, can be computed from the ratio of activities found in the two absorbers, provided that t_s and t_0 are known.

C. Source and Overcoating Thickness Determinations

The source and overcoating thicknesses were measured by a method which takes advantage of the known absorption behavior of the alpha particles from the Ra target itself. The method consisted essentially of masking each target face down to the same area as was effective during the fission runs and counting the number of alpha particles which succeed in penetrating various thicknesses of absorber. In this way, a plot of $N(>t)$ vs t was obtained. If the alpha particles are well collimated in a direction perpendicular to the source face ($\theta=0$), the θ variable disappears from Eqs. (1) and (2), leaving

$$N(>t)=k'\int_0^{n'R'} dx=k'n'R', \tag{10}$$

and

$$N(>t)=k'\int_0^{R'-t} dx=k'(R'-t) \tag{11}$$

in Regions I and II, respectively, where the primed quantities denote alpha-particle parameters. From Eqs. (10) and (11) it can be seen that the experimentally determined plot of $N(>t)$ vs t for collimated monoenergetic alphas should have the identical shape and abscissa position as the $-dN/dt$ vs t plot given in Fig. 4(b) for a 2π or stacked-foil geometry, including the effects of range straggling. The source thickness t_s can then be determined graphically from the experimental plot. The overcoating thickness t_0 is simply the difference between the graphical value of R' and the known range of the alpha particle. In the experiment, the source and detector were placed at opposite ends of a chamber 52 cm in length which could be filled with various pressures of air, allowing the convenient choice of any absorber "thickness." The air pressures were

then converted to equivalent thicknesses of Au by the application of well-known stopping-power data.[8,10] Ra^{226} and its daughters emit several groups of alpha particles. Fortunately, however, the most penetrating group, from Po^{214} (RaC′) at 7.680 Mev, is well separated in energy from the others and could therefore be used as the subject of the range measurements.

An experimental, background-corrected alpha-particle absorption curve for one of the target faces is shown in Fig. 5, in which the first drop-off corresponds to absorption of the unresolved low-energy alpha particles. From the absorption curve t_s and t_0 were determined graphically and converted to Au equivalent. The alpha absorption method was checked with a thin Cm^{244} source, whose measured range agreed with the value of reference 10 to within 1.4%.

IV. RESULTS AND DISCUSSION

A. Relative Yields

If the angular anistropy of fission in the system of the fissioning nucleus is small and/or symmetric about 90°, and if η is indeed negligible as indicated above, then one may assume that the numbers of forward- and backward-hemisphere fragments are equal within experimental error. The recoil direction may then be disregarded in the yield experiments, and differences may be ascribed solely to differences in energy of the protons incident on each target face. This assumption is supported by the fact that the yields determined in this way fall, within experimental error, on smooth curves when plotted against proton energy regardless of whether they are forward or backward yields.

The relative yields were determined by counting the appropriate activities found in foils IC_1, a_1+b_1, IC_2, and a_2+b_2 of Fig. 3(b). The foil thicknesses in the stack were such that the nominal incident proton energies at the target faces feeding these catchers were 22.1, 20.3, 13.6, and 11.0 Mev, respectively. The activities were corrected for the different amounts of Ra in the target faces, as determined by alpha counting. They were also corrected for the thickness parameters of their respective target faces by substituting for R, t, and nR in Eq. (3) the measured values of R, t_0, and t_s, respectively.

The corrected yields are given in Table I and are plotted in Fig. 6. The yield of each fragment is normalized to unity at 13.6 Mev. It is apparent that the symmetric fission yield, typified by Pd^{112}, rises faster with proton energy than does the asymmetric or Sr^{91} yield. Since the symmetric and asymmetric peaks have been found[1] to be of approximately the same height at 11 Mev, symmetric fission evidently predominates at

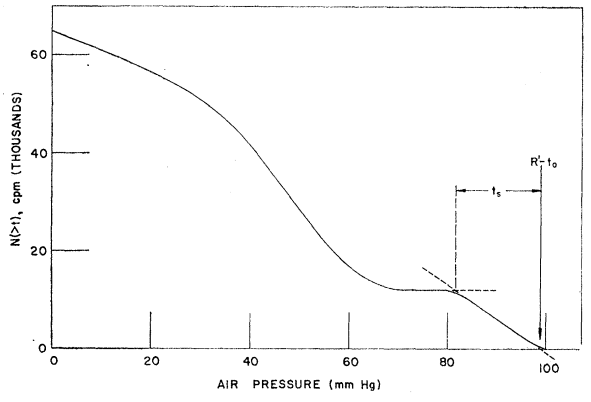

FIG. 5. Absorption of alpha particles from one of the targets. The first drop-off corresponds to the unresolved ranges of the low-energy alphas from Ra^{226} and its daughters. The second drop-off gives the residual range of the 7.68-Mev Po^{214} alpha particle. The source thickness t_s is obtained graphically, as shown. The overcoating thickness t_0 is obtained by subtracting $R'-t_0$ from the known range R' of the Po^{214} alpha particle.

[10] H. A. Bethe and J. Ashkin, in *Experimental Nuclear Physics*, edited by E. Segrè (John Wiley & Sons, Inc., New York, 1953), Vol. 1.

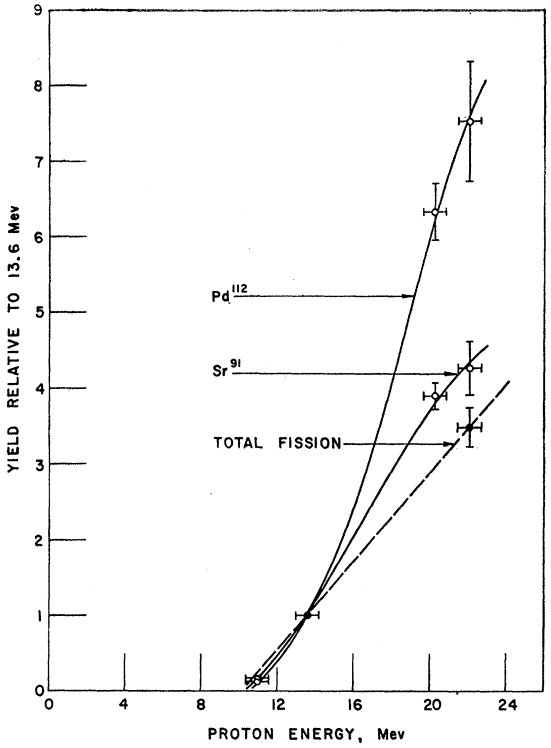

FIG. 6. Relative yields of Sr^{91}, Pd^{112}, and total fission as a function of proton energy.

TABLE I. Relative yields.[a]

	Proton energy in Mev			
	11.0	13.6	20.3	22.1
Sr^{91}	0.15±0.01	1.00	3.90±0.17	4.26±0.35
Pd^{112}	0.13±0.01	1.00	6.33±0.38	7.53±0.79
(p,f)	···	1.00	···	3.49±0.26

[a] Relative to the 13.6-Mev yield of each process. Errors are standard deviations.

TABLE II. Ranges and energies of fragments.

		Proton energy, Mev 11	20
Range, mg Au/cm^2	Sr^{91}	11.2±0.9	10.8±0.2
	Pd^{112}	9.1±1.0	9.2±0.3
Energy,[a] Mev	Sr^{91}	106±32	100±7
	Pd^{112}	80±32	81±10

[a] Assuming $R \propto E^{\frac{3}{2}}$ and proportionality constants of reference 13.

higher energies, as might be expected from fission systematics. The symmetric and asymmetric peak heights differ appreciably only above ~14 Mev. The possibility that the Sr^{91} and Pd^{112} curves cross over below 14 Mev, reflecting an asymmetric, two-humped mass yield curve at lower energies, appears unlikely from the present data. The question of whether the mass-yield curve at 22 Mev is still triple-humped or has evolved into a single peak remains to be answered by the determination of valley yields.

The dashed curve in Fig. 6 was obtained by counting total fission activity from the catcher foils without chemical separation. These yields have been corrected for the amounts of Ra in the targets but not for t_0, t_s, and R, since the range behavior of gross fission fragments was not investigated. Since the t_0, t_s, and R corrections were small (<6%) for Sr^{91} and Pd^{112}, however, the general trend of the total fission yield curve is probably correct. Its relatively slow rise with increasing proton energy indicates that the mass-yield curve may become narrower at higher energies. The slope of the curve of total fission yield vs energy between 13.6 and 22.1 Mev is the same as has been found[11] for the fast-neutron-induced fission of Ra^{226}. All three yield curves show an apparent fission threshold at about 10.4 Mev.

B. Ranges

The ranges of Sr^{91} and Pd^{112} fragments were computed by means of Eq. (9) from the results of three to five duplicate integral runs at each proton energy. These results were averaged with those of two or three differential runs made at the higher proton energy. Agreement between the differential and integral runs was good. The average ranges[12] and their standard deviations are given in Table II. If the range is proportional to the two-thirds power of the fragment kinetic energy, and if proportionality constants of 0.50 and 0.49 [13] (ranges in mg Au/cm^2, energies in Mev) are used for Sr^{91} and Pd^{112}, respectively, the ranges correspond to the energies shown in Table II. The large standard deviations on the 11-Mev range values result from the small cross section and from the fragment losses inherent in recoil-catching methods. The kinetic energy precision is further reduced by the three-halves-power dependence on range.

From the values in Table II an average total kinetic energy $\bar{E}_k$ (both fragments) of 162±10 Mev is obtained for 20-Mev protons on Ra^{226}. This value falls, within experimental error, on the curve of $\bar{E}_k$ vs $Z^2/A^{\frac{1}{3}}$ of the fissioning nucleus, which has been shown by Terrell[14] to correlate a wide variety of fissioning nuclei.

Fragment kinetic energies, while reflecting variations in such fission parameters as primary fragment distortion energies, are not very sensitive indicators and must be measured to precisions of 2% or better in order to show the effects of any likely changes in mechanism. Therefore, although the present range data show no large changes in the distribution of fission energy as the proton energy is varied, changes in distortion energy and/or the identity of the average fissioning nucleus are not precluded.

ACKNOWLEDGMENTS

The author is indebted to Dr. N. Sugarman for aid with some of the range derivations and to Dr. J. L. Need and the staff of the ORNL 86-inch cyclotron for arranging the irradiations.

[11] R. A. Nobles and R. B. Leachman, Nuclear Phys. **5**, 211 (1958).

[12] The values in Table I differ from those reported earlier [R. L. Wolke, Bull. Am. Phys. Soc. 4, 414 (1959)] because the latter were uncorrected for source thickness effects.

[13] Interpolated from data of J. Alexander (private communication).

[14] J. Terrell, Phys. Rev. **113**, 527 (1959).